Kerr-lens mode-locking of an Yb:CLNGG laser

Zhang-Lang Lin, Pavel Loiko, Huang-Jun Zeng, Wen-Ze Xue, Ge Zhang, Simone Normani, Patrice Camy, Valentin Petrov, Xavier Mateos, Haifeng Lin, et al.

Research Article Vol. 31, No. 5 / 27 Feb 2023 / Optics Express 8575
Optics EXPRESS

Kerr-lens mode-locking of an Yb:CLNGG laser

Zhang-Lang Lin,[1] Pavel Loiko,[2] Huang-Jun Zeng,[1] Wen-Ze Xue,[1] Ge Zhang,[1] Simone Normani,[2] Patrice Camy,[2] Valentin Petrov,[3] Xavier Mateos,[4] Haifeng Lin,[5] Haohai Yu,[6] Huaijin Zhang,[6] Junhai Liu,[7] Li Wang,[3] and Weidong Chen[1,3,*]

[1] *Fujian Institute of Research on the Structure of Matter, Chinese Academy of Sciences, 350002 Fuzhou, China*
[2] *Centre de Recherche sur les Ions, les Matériaux et la Photonique (CIMAP), UMR 6252 CEA-CNRS-ENSICAEN, Université de Caen, 6 Boulevard Maréchal Juin, 14050 Caen Cedex 4, France*
[3] *Max Born Institute for Nonlinear Optics and Short Pulse Spectroscopy, Max-Born-Str. 2a, 12489 Berlin, Germany*
[4] *Universitat Rovira i Virgili, URV, Física i Cristal·lografia de Materials, FiCMA, Marcel·lí Domingo 1, 43007 Tarragona, Spain*
[5] *College of Physics and Optoelectronic Engineering, Shenzhen University, 518118 Shenzhen, China*
[6] *State Key Laboratory of Crystal Materials, Shandong University, 250100 Jinan, China*
[7] *College of Physics, Qingdao University, 266071 Qingdao, China*
[*] *chenweidong@fjirsm.ac.cn*

Abstract: We report on a Kerr-lens mode-locked laser based on an Yb^{3+}-doped disordered calcium lithium niobium gallium garnet (Yb:CLNGG) crystal. Pumping by a spatially single-mode Yb fiber laser at 976 nm, the Yb:CLNGG laser delivers soliton pulses as short as 31 fs at 1056.8 nm with an average output power of 66 mW and a pulse repetition rate of ~77.6 MHz via soft-aperture Kerr-lens mode-locking. The maximum output power of the Kerr-lens mode-locked laser amounted to 203 mW for slightly longer pulses of 37 fs at an absorbed pump power of 0.74 W, which corresponds to a peak power of 62.2 kW and an optical efficiency of 20.3%.

1. Introduction

Calcium niobium gallium garnets (CNGG) are promising host materials for doping with trivalent laser-active rare-earth ions such as ytterbium (Yb^{3+}) [1,2]. Their main advantage is the strong inhomogeneous broadening of absorption and emission bands of the dopant ions arising from the structure disorder [3]. CNGG crystals belong to the crystal family of cubic (sp. gr. $Ia\bar{3}d$) multicomponent garnets $\{A\}_3[B]_2(C)_3O_{12}$, with {A}, [B], and (C) standing for dodecahedral, octahedral, and tetrahedral lattice sites, respectively (a stoichiometric crystal has the chemical formula $\{Ca_3\}[Nb_{1.5}Ga_{0.5}](Ga_3)O_{12}$ [4]). For a congruent crystal, the Nb^{5+} and Ga^{3+} cations are randomly distributed over both the [B] and (C) sites, and cationic vacancies appear to maintain charge neutrality, so that the dopant rare-earth ions replacing for the Ca^{2+} cations experience a number of second coordination spheres [1]. Owing to this, Yb^{3+}-doped CNGG crystals feature broad and smooth emission bands at ~1 μm, as compared to ordered garnets such as $Y_3Al_5O_{12}$ (YAG), making the former materials promising for broadly tunable and especially femtosecond (fs) mode-locked (ML) lasers [5–7]. The structure disorder leads to a certain drop in the thermal conductivity of CNGG (4.3 $Wm^{-1}K^{-1}$ at room temperature [1]).

The material engineering of Yb:CNGG targets (i) the elimination of cationic vacancies causing color centers formation responsible for a parasitic broadband absorption (crystal coloration) and (ii) tailoring the emission band of Yb^{3+} ions [3,8]. The cationic vacancies can be removed by introducing charge compensators, such as univalent alkali metal cations (Na^+ or Li^+; the host

#480986 https://doi.org/10.1364/OE.480986
Journal © 2023 Received 22 Nov 2022; revised 1 Feb 2023; accepted 6 Feb 2023; published 22 Feb 2023

Optics EXPRESS

matrix is then abbreviated as CNNGG and CLNGG, respectively). In addition to the improvement of the optical quality, such Na^+ / Li^+ codoping may also contribute to an additional spectral line broadening for the Yb^{3+} transition.

Yb^{3+}-doped CNGG-type laser crystals provide broad, smooth and flat gain profiles slightly above 1 μm supporting the generation of sub-100 fs pulses in the ML operation regime. Schmidt *et al.* reported on an Yb:CNGG laser ML by a SEmiconductor Saturable Absorber Mirror (SESAM) delivering 73 fs pulses at a central wavelength of 1047.5 nm with an average output power of 46 mW [5]. Zhang *et al.* employed a single-walled carbon nanotube saturable absorber (SWCNT-SA) for mode-locking of an Yb:CLNGG laser generating 90 fs pulses at 1049 nm with an average output power of 20 mW [6]. In these studies, Ti:Sapphire laser pumping was used. Pumping by a high-brightness distributed Bragg reflector (DBR) tapered diode laser at 979 nm, 55 fs pulses were obtained at 1051.5 nm from a SESAM ML Yb:CLNGG laser [7]. So far, the shortest pulse duration for any Yb^{3+}-doped CNGG-type crystal was achieved from a diode-pumped SESAM ML Yb:CNNGG laser which generated pulses as short as 45 fs at 1061 nm (after external compression using a pair of Brewster prisms, 62 fs directly from the oscillator) [9].

The optical Kerr effect is an instantaneous variation of the refractive index of a material caused by the electric field of a light wave. Such a refractive index variation is proportional to the intensity of the electric field, $\Delta n = n_2 I$, where n_2 is the coefficient representing the nonlinear refractive index part. It becomes relevant for high-intensity / short-pulse laser beams and creates an optical phase delay / wavefront deformation similar to the action of a lens (the so-called Kerr lens). For materials with $n_2 > 0$, the spatial effect is also referred to as self-focusing. Kerr-lens mode locking (KLM) is a technique of passive mode-locking of a laser using an artificial saturable absorber relying on the Kerr lensing in the gain medium which is equivalent to a nonlinear loss rather than absorption. In the case of soft-aperture KLM, the Kerr lens creates a better overlap of the laser and pump modes in the gain medium leading to higher gain for shorter pulses. KLM benefits from a fast response time facilitating the generation of ultrashort (down to few optical cycles) pulses and the lack of bandwidth limitation inherent to physical saturable absorbers [10]. Ultrashort (sub-50 fs) pulses were generated from Kerr-lens mode-locked bulk Yb lasers employing different structurally disordered laser crystals [11–16]. However, up to date, there are no reports on KLM of lasers based on Yb^{3+}-doped CNGG-type garnets. Note that CNGG like other gallium garnets is expected to be a promising Kerr medium with a high n_2 value [17].

In the present work, we aimed to further shorten the pulse duration in lasers based on Yb^{3+}, Li^+-codoped CNGG crystals via soft-aperture Kerr-lens mode-locking.

2. Spectroscopic properties of Yb:CLNGG

An Yb^{3+}, Li^+-codoped calcium niobium gallium garnet crystal (Yb:CLNGG) with a starting composition of $(Ca_3Li_{0.275}Nb_{1.775}Ga_{2.95}O_{12})_{0.95}(Yb_3Ga_5O_{12})_{0.05}$ (5 at.% Yb^{3+} doping) was grown by the conventional Czochralski method. The actual Yb^{3+} doping level was measured to be 4.3±0.3 at.% (Yb^{3+} ion density: $N_{Yb} = 5.75 \times 10^{20}$ at/cm^3). Li^+ addition reduces the segretation coefficent of Yb^{3+} ions in CNGG crystals [3] while playing a positive role in their quality.

The as-grown crystal was colorless and transparent, Fig. 1(a). The absorption at ~1 μm is due to the $^2F_{7/2} \rightarrow {}^2F_{5/2}$ Yb^{3+} transition. The UV absorption edge appeared at 295 nm. A very weak and broad absorption band centered at ~410 nm is assigned to color centers associated with residual cationic vacancies.

The Raman spectrum of the Yb:CLNGG crystal is shown in Fig. 1(b). Two structured bands at high phonon energies are assigned to symmetric stretching modes (ν_s) of isolated metal-oxygen tetrahedra [$M2O_4$] where M2 stands for cations (Ga^{3+} and Nb^{5+}) in (C) lattice sites [18]. For the low energy band related to [$Ga2O_4$], the lines at 776 and 748 cm^{-1} are the fingerprints of undistorted tetrahedra and cationic vacancies, respectively. For the high energy band, the lines at

Optics EXPRESS

827 and 849 cm^{-1} in a similar way represent the [$Nb2O_4$] tetrahedra. The latter line is very weak in the Raman spectrum of Yb:CLNGG indicating the role of Li^+ codoping for the local charge compensation in tetrahedral sites [3].

The room temperature (RT, 293 K) absorption cross-section, σ_{abs}, of Yb:CLNGG is shown in Fig. 1(c). For the zero-phonon line (ZPL), the peak σ_{abs} is 1.84×10^{-20} cm^2 at 972.2 nm and the corresponding bandwidth (full width at half maximum, FWHM) is relatively broad, 3.1 nm, making this material suitable for pumping with commercial high-power InGaAs diode lasers for power scalable operation. At shorter wavelengths, σ_{SE} is lower, 0.67×10^{-20} cm^2 at 943.7 nm, while corresponding to much broader absorption peaks. The determined σ reasonably agree with the previous studies [1,3] considering the error in the measured concentration of Yb^{3+}ions. The RT stimulated-emission (SE) cross-sections, σ_{SE}, were calculated using a combination of the reciprocity method and the Füchtbauer–Ladenburg equation, see Fig. 1(c). In the spectral range where laser operation is expected (i.e., at wavelengths above the ZPL), the maximum σ_{SE} is 1.13×10^{-20} cm^2 at ~1027 nm.

Figure 1(d) shows a RT luminescence decay curve measured using a finely powdered sample to avoid the effect of radiation trapping (reabsorption). The decay is single-exponential and the luminescence lifetime τ_{lum} is 0.782 ms. This value is slightly longer than the estimate for the radiative lifetime obtained from a comparison of σ_{SE} spectra derived by the two methods, $\tau_{rad} = 0.65 \pm 0.05$ ms. This estimate is within the range of luminescence lifetimes of Yb^{3+} ions in a 0.3 at.% Yb:CNGG crystal at 6 K reported by Serrano et al. [3], 0.6 – 0.8 ms, depending on the nature of a particular Yb^{3+}center.

According to the quasi-three-level nature of the Yb laser scheme with inherent reabsorption, the RT gain cross-sections, $\sigma_{gain} = \beta\sigma_{SE} - (1 - \beta)\sigma_{abs}$, were calculated to derive the gain spectra shown in Fig. 1(e). Here, $\beta = N_2/N_{Yb}$ is the inversion ratio and N_2 is the population of the upper laser level ($^2F_{5/2}$). The gain profiles are smooth and very broad extending until up to at least 1.15 µm owing to a profound phonon sideband. With increasing the inversion ratio β from 0.02 to 0.12 results in a monotonous blue-shift of the local gain maximum from 1067 to 1030 nm. For a β value of 0.06, the gain FWHM amounts to ~29 nm.

The low-temperature (LT, 12 K) absorption and emission spectra of Yb^{3+} ions in CLNGG are shown in Fig. 1(f). The Yb^{3+} ions in CNGG-type crystals replace for the Ca^{2+} cations in sites with a D_2 symmetry and VIII-fold oxygen coordination. Each $^{2S+1}L_J$ Yb^{3+} multiplet is split into a total of 2J + 1 sub-levels which are determined as follows: $^2F_{7/2}$ = (0, 353, 522 and 761 cm^{-1}) and $^2F_{5/2}$ = (10298, 10710, and 10851 cm^{-1}). Here, the Stark level assignment follows previous work [19]. The corresponding partition functions at RT are $Z_1 = 1.277$ and $Z_2 = 1.198$ and their ratio $Z_1/Z_2 = 1.066$. At 12 K, the ZPL has a maximum at 10298 cm^{-1} (due to [YbO_8] dodecahedra surrounded by [GaO_4] tetrahedra) and a shoulder at 10286 cm^{-1} (assigned to Li^+ substitution in the tetrahedral sites) [3]. A similar complex ZPL structure is also found in the LT emission spectra.

Optics EXPRESS

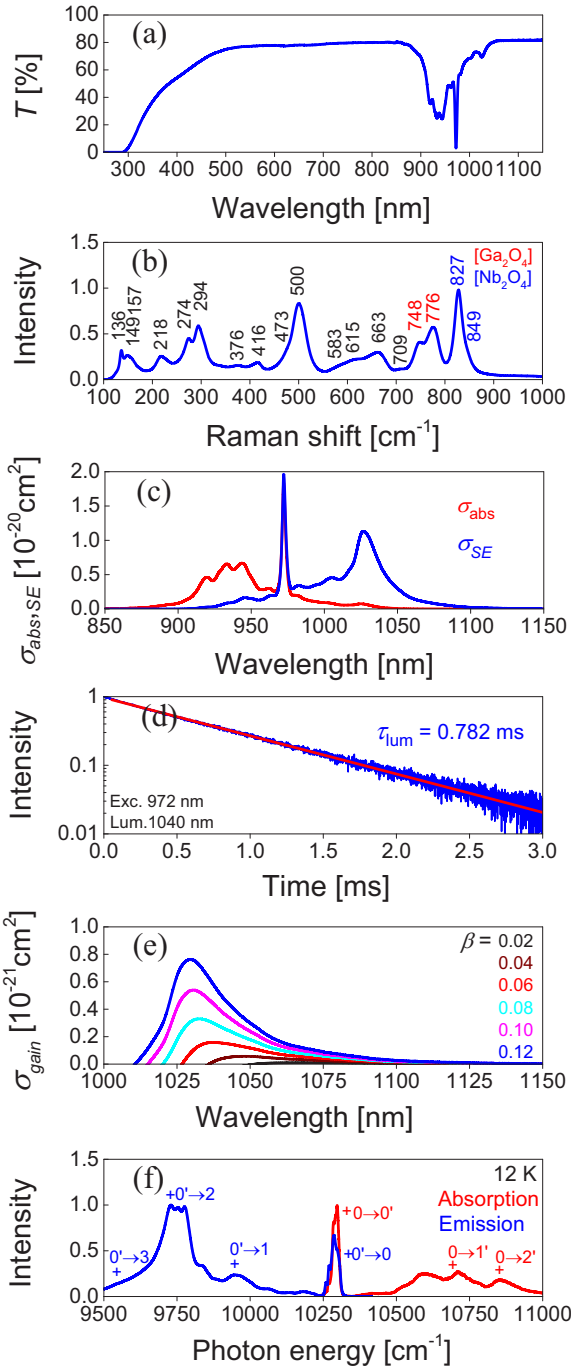

Fig. 1. Spectroscopic characterization of the Yb:CLNGG crystal: (a) transmission spectrum (thickness: 3.1 mm); (b) Raman spectrum, $\lambda_{exc} = 514$ nm, *numbers* – phonon energies; (c) RT absorption, σ_{abs} and SE, σ_{SE}, cross-sections; (d) RT luminescence decay measured with powdered sample, *symbols* – experimental data, *line* – single-exponential fit, $\lambda_{exc} = 972$ nm, $\lambda_{lum} = 1040$ nm; (e) gain cross-sections, σ_{gain}, for different inversion ratios β; (f) LT (12 K) absorption and emission spectra, "+" indicate electronic transitions.

Optics EXPRESS

3. Laser set-up

An X-shaped astigmatically compensated standing-wave cavity was used for studying the laser performance of the Yb:CLNGG crystal, as shown in Fig. 2. A 2.18-mm thick sample was cut from the as-grown bulk 5 at.% Yb^{3+}-doped CLNGG crystal along the [111] crystallographic direction with an aperture of 3.3×3.3 mm^2. It was mounted in a water-cooled copper holder (coolant temperature: 17°C) and placed at Brewster's angle between two concave dichroic folding mirrors M_1 and M_2 (radius of curvature: RoC = -100 mm) with the minimum loss condition fulfilled for both the pump and laser wavelengths. The pump source was a CW Yb fiber laser with a linearly polarized narrow-linewidth (~50 kHz) output at 976 nm. It emitted a nearly diffraction-limited beam with a measured beam propagation factor (M^2) of ~1.03. The pump beam was focused into the laser crystal through the dichroic mirror M_1 by a spherical focusing lens with a focal length of 75 mm, which resulted in a beam waist (radius) of 15.5 µm × 35.5 µm in the sagittal and tangential planes, respectively.

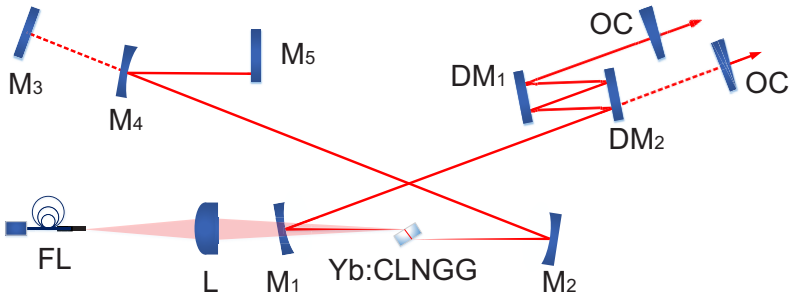

Fig. 2. Experimental layout of the Yb:CLNGG laser. FL: Yb fiber laser emitting at 976 nm; L: spherical focusing lens; M_1, M_2 and M_4: concave mirrors (RoC = -100 mm); M_3 and M_5: flat end mirrors; DM_1 and DM_2: flat dispersive mirrors; OC: output coupler.

For CW laser experiments, a four-mirror cavity was used. One cavity arm was terminated by a flat rear mirror M_3 and the other arm – by a plane-wedged output coupler (OC) with a transmission at the laser wavelength T_{OC} ranging from 1% to 10%. The cavity mode inside the laser crystal was simulated using the ray transfer matrix (ABCD) formalism yielding a waist radius of 22 µm × 44 µm in the sagittal and the tangential planes, respectively. The measured single-pass pump absorption under lasing conditions decreased with the transmission of the OC from 32.5% to 27.6% indicating some absorption saturation / recovery. The weak pump absorption efficiency was mainly due to the low absorption cross-sections of Yb:CLNGG.

For KLM operation, the flat end mirror M_3 was substituted by a curved mirror M_4 (RoC = -100 mm) and the cavity arm was terminated by a flat rear mirror M_5. The intracavity group delay dispersion (GDD) management was carried out by implementing two flat dispersive mirrors (DMs) characterized by a GDD per bounce of $DM_1 = DM_2 = -200$ fs^2. The resulting total round-trip negative GDD amounted to -1600 fs^2 to compensate the material dispersion and to balance the self-phase modulation (SPM) induced by the Kerr nonlinearity of the laser crystal. The round-trip material dispersion was estimated from the dispersion curve of a similar CNGG crystal [1] to be ~+673 fs^2 at 1050 nm. The physical length of the ML cavity was 1.93 m which corresponds to a pulse repetition rate of ~77.6 MHz.

4. Results and discussion

4.1. Continuous-wave laser operation

In the CW regime, a maximum output power of 666 mW was achieved at 1037.6 nm with a slope efficiency η as high as 80.6% (*vs.* the absorbed pump power) and a laser threshold of 184 mW

Optics EXPRESS

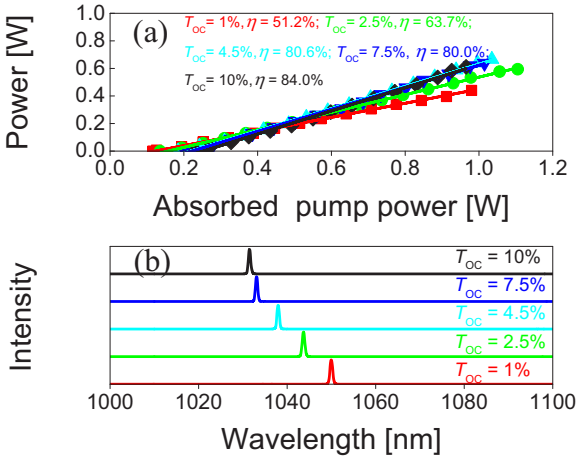

Fig. 3. CW Yb:CLNGG laser: (a) Input-output dependences for different OCs, η – slope efficiency; (b) Typical spectra of the laser emission.

(using $T_{OC} = 4.5\%$). This corresponds to an absorbed pump power of 1.035 W and an optical efficiency of 64.3%, see Fig. 3(a). Even higher η of 84% was obtained with a 10% OC reaching 611 mW at 1031.4 nm at an absorbed power of 0.97 W. The obtained laser slope efficiencies for high output coupling values are close to the Stokes limit under lasing conditions indicating low losses in the laser crystal (see below). The laser threshold gradually increased with the output coupling, from 116 mW ($T_{OC} = 1\%$) to 231 mW ($T_{OC} = 10\%$). The laser wavelength in the CW regime experienced a monotonic blue-shift with increasing OC transmission, from 1050.0 to 1031.4 nm, as shown in Fig. 3(b). This behavior is typical for quasi-three-level Yb lasers with inherent reabsorption at the laser wavelength. It also agrees well with the calculated gain spectra of Yb:CLNGG, cf. Figure 1(b).

To determine the parasitic losses in the Yb:CLNGG crystal, we have applied the Caird analysis: the measured laser slope efficiency was fitted as a function of -ln(R_{OC}), where $R_{OC} = 1 - T_{OC}$ is the output coupler reflectivity [19]. The analysis yielded total round-trip cavity losses of $\delta = 0.8 \pm 0.2\%$ (reabsorption losses excluded) and an intrinsic slope efficiency η_0 of $93 \pm 3\%$, as shown in Fig. 4(a). This corresponds to a passive loss coefficient of 0.002 cm^{-1} which is close to values for ordered gallium garnets such as Yb:YGG [20].

The potential of the Yb:CLNGG crystal for broad wavelength tuning was studied in the CW regime by inserting a 2-mm thick quartz plate (a Lyot filter) at Brewster's angle acting as a Lyot filter close to the OC ($T_{OC} = 0.4\%$) at an incident pump power of 1 W. The laser wavelength was continuously tunable between 1012 and 1082 nm, i.e., across 70 nm at the zero-power-level, see Fig. 4(b). The tuning curve was simulated using a simple analytical model of a quasi-three-level laser [21] using the cavity parameters and the spectroscopic properties of Yb^{3+} ions in the CLNGG crystal described above. The calculated curve is in good agreement with the measured one.

4.2. *Kerr-lens mode-locked laser operation*

The KLM operation of the Yb:CLNGG laser was first investigated using a 2.5% OC at an absorbed pump power of 1 W. To discriminate the CW regimes, the laser cavity was aligned towards the edge of the stability region via translating the folding mirror (M_2) away from the pump mirror (M_1) step by step, which resulted in a significant drop of the CW output power. After careful cavity alignment, KLM operation could be initiated by slightly knocking the OC or translating the flat rear mirror M_5. When mode-locked, the Yb:CLNGG laser experienced

Optics EXPRESS

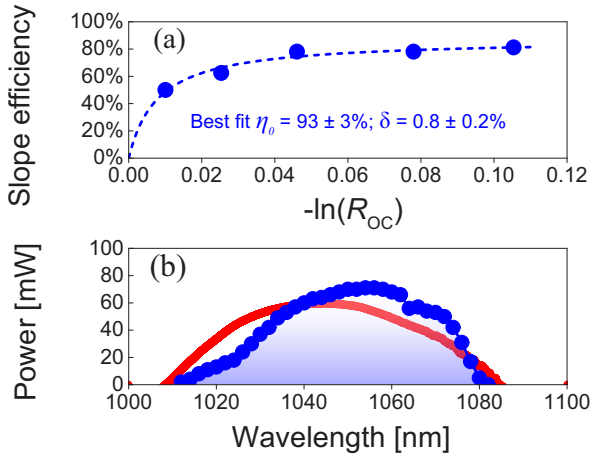

Fig. 4. CW Yb:CLNGG laser: (a) Caird analysis: laser slope efficiency plotted *vs.* -ln(R_{OC}); where $R_{OC} = 1 - T_{OC}$; (b) Tuning curve obtained with a Lyot filter and a 0.4% OC (*symbols* – experimental data, *curve* – simulation).

an abrupt increase of the output power from 145 to 203 mW. The measured optical spectrum of the laser pulses plotted both in linear and logarithmic (inset) scales is shown in Fig. 5(a). It has an emission bandwidth (FWHM) of 33.7 nm at a central wavelength of 1056.6 nm by assuming a sech^2-shaped spectral profile. The recorded interferometric autocorrelation trace gave a deconvolved pulse duration of 37 fs (FWHM) again assuming a sech^2-shaped temporal pulse profile, see Fig. 5(b). The corresponding time-bandwidth product (TBP) of 0.335 was slightly above the Fourier-transform-limit (0.315). A long-scale background-free intensity autocorrelation scan (50 ps) confirmed the single-pulse steady-state mode-locking, see the inset in Fig. 5(b). An average output power of 203 mW was obtained at an absorbed pump power of 1 W, corresponding to an optical efficiency of 20.3% and a peak power of 62.2 kW. In this case, the on-axis peak intensity in the Yb:CLNGG crystal amounted to 332 GW/cm^2.

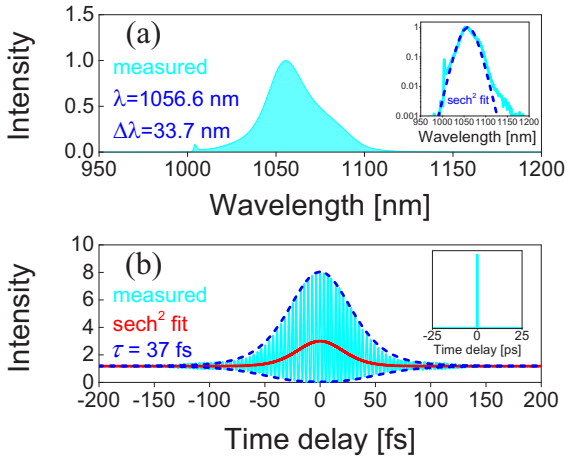

Fig. 5. KLM Yb:CLNGG laser with $T_{OC} = 2.5\%$. (a) Optical spectrum, linear scale (*inset* – logarithmic scale, *dashed curve* – sech^2 fit); (b) interferometric autocorrelation trace, *red curve* - sech^2 fit. *Inset*: intensity autocorrelation trace measured on a time span of 50 ps.

Optics EXPRESS

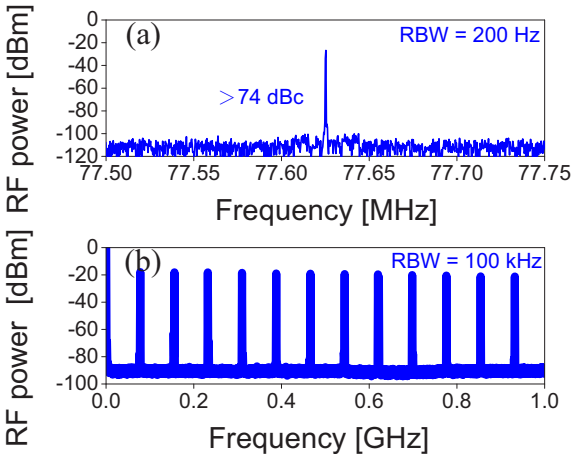

Fig. 6. RF spectra of the KLM Yb:CLNGG laser with $T_{OC} = 2.5\%$: (a) Fundamental beat note at 77.63 MHz recorded with a resolution bandwidth (RBW) of 200 Hz, and (b) harmonics on a 1-GHz frequency span recorded with a RBW of 100 kHz.

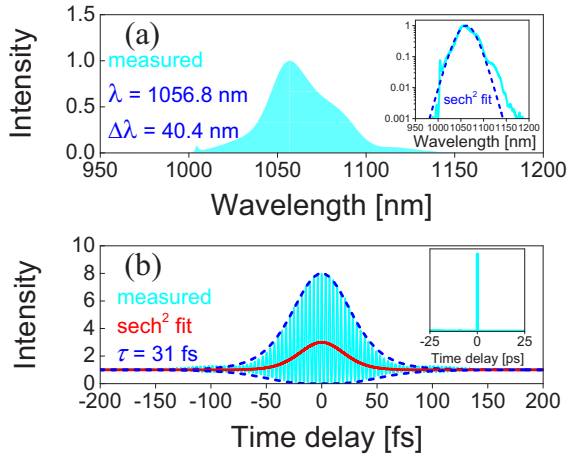

Fig. 7. KLM Yb:CLNGG laser with $T_{OC} = 1.6\%$. (a) Optical spectrum, linear scale (*inset* – logarithmic scale, *dashed curve* – sech^2 fit); (b) interferometric autocorrelation trace, *red curve* - sech^2 fit. *Inset*: intensity autocorrelation trace measured on a time span of 50 ps.

A radio-frequency (RF) spectrum analyzer was used for confirming the stability of the KLM operation. A relatively high extinction ratio of >74 dBc above the noise level for the fundamental beat note at 77.63 MHz in combination with the uniform harmonics recorded on a 1-GHz frequency span provided evidence of highly stable CW-ML operation without any Q-switching or multi-pulsing instabilities, see Fig. 6.

The shortest pulses with ultimate stability were achieved by reducing the transmittance of the OC down to 1.6%. The characterization of these laser pulses is shown in Fig. 7. The measured laser spectrum, plotted again both in linear and logarithmic scales, is shown in Fig. 7(a). Assuming a sech^2-shaped spectral profile [see the inset in Fig. 7(a)], the KLM laser delivered pulses having a broader spectral bandwidth of 40.4 nm centered at 1056.8 nm. The pulse duration was estimated from the recorded interferometric autocorrelation trace, as shown in Fig. 7(b). The curve was well fitted with a sech^2-shaped temporal profile, yielding an estimation of 31 fs (~9

Optics EXPRESS

optical cycles) for the pulse duration. The corresponding TBP was 0.336 being only slightly above the Fourier-transform-limit. The inset in Fig. 7(b) shows the measured background-free intensity autocorrelation trace on a long-time span of 50 ps indicating single-pulse CW-ML operation free of multiple pulse instabilities. The average output power for the shortest pulses amounted to 66 mW at an absorbed pump power of 0.74 W, corresponding to an optical efficiency of 8.9% and a peak power of 24.1 kW. For this OC, the estimated peak on-axis intensity in the crystal was lower, 197 GW/cm^2.

The RF spectra of the shortest pulses are recorded to verify the ultimate stability of the ML operation in different frequency span ranges, as shown in Fig. 8. The recorded first beat note located at 77.63 MHz exhibited yet higher extinction ratio of >77 dBc above carrier and the harmonics were similarly uniform as recorded on the 1-GHz frequency span.

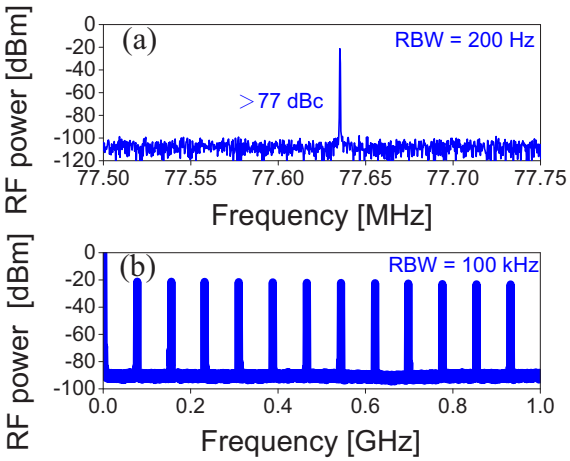

Fig. 8. RF spectra of the KLM Yb:CLNGG laser with $T_{OC} = 1.6\%$: (a) Fundamental beat note at 77.63 MHz recorded with a RBW of 200 Hz, and (b) Harmonics on a 1-GHz frequency span recorded with a RBW of 100 kHz.

High-peak intensities in the laser crystal are expected to a noticeable modification of the spatial profile of the laser beam owing to the Kerr lens effect. This was confirmed by monitoring the far-field beam profiles both for the CW and KLM regimes with an IR camera placed at ~1.2 m away from the OC ($T_{OC} = 1.6\%$). The transition from CW to dominating soft-aperture KLM was accompanied by a significant shrinking of the beam diameter from 2.86 mm (x) × 2.08 mm (y) to 2.07 mm (x) × 2.09 mm (y), as shown in Fig. 9. Gallium-containing garnets are known to exhibit relatively high n_2 values (in agreement with their large linear refractive indices). Indeed, for $Gd_3Ga_5O_{12}$ (GGG), $n_2 = 1.3 \times 10^{-19}$ m^2/W which is higher than for YAG, $n_2 = 0.62 \times 10^{-19}$ m^2/W (the values are specified at 1 µm) [17]. No direct measurements of n_2 for CNGG are reported in the literature. Using the model of Boling, Glass, and Owyoung (BGO) [22], we calculated n_2 of CNGG to be 2.1×10^{-19} m^2/W at 1 µm. This value reasonably agrees with the estimation of Pan *et al.* from the soliton mode-locking theory, 1.1×10^{-19} m^2/W at ~2 µm [23], considering the dispersion of n_2 in the near-infrared.

Optics EXPRESS

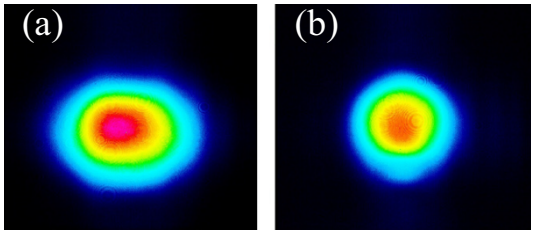

Fig. 9. Measured far-field beam profiles of the Yb:CLNGG laser: (a) CW and (b) KLM regimes of operation, $T_{OC} = 1.6\%$.

5. Conclusion

To conclude, Yb^{3+}-doped calcium niobium gallium garnet (Yb:CLNGG) is a promising crystal for Kerr-lens mode-locked lasers emitting few-optical-cycle pulses at ~1 µm. This is due to its advantageous spectroscopic properties, namely smooth and very broad gain spectra owing to the strong inhomogeneous spectral broadening arising from the structure disorder, and relatively high nonlinear refractive index. In the present work, a soft-aperture Kerr-lens mode-locked Yb:CLNGG laser pumped by a spatially single-mode Yb fiber laser at 976 nm delivered soliton pulses as short as 31 fs at a central wavelength of 1056.8 nm with an average output power of 66 mW at a repetition rate of 77.63 MHz. The average output power was scaled to 203 mW using an output coupler with a higher transmission at the expense of a slightly longer pulse duration (37 fs).

Funding. National Key Research and Development Program of China (2021YFB3601504); National Natural Science Foundation of China (61975208, 61905247, U21A20508); Sino-German Scientist Cooperation and Exchanges Mobility Program (M-0040); MCIN/AEI (PID2019-108543RB-I00).

Acknowledgment. Xavier Mateos acknowledges the Serra Húnter program.

Disclosures. The authors declare no conflicts of interest.

Data availability. Data underlying the results presented in this paper are not publicly available at this time but may be obtained from the authors upon reasonable request.

References

1. E. C. Hernandez, M. D. Serrano, R. J. J. Rioboo, C. Cascales, and C. Zaldo, "Na Modification of Lanthanide Doped Ca3Nb1.5Ga3.5O12-Type Laser Garnets: Czochralski Crystal Growth and Characterization," Cryst. Growth Des. **16**(3), 1480–1491 (2016).
2. J. Liu, Y. Wan, Z. Zhou, X. Tian, W. Han, and H. Zhang, "Comparative study on the laser performance of two Yb-doped disordered garnet crystals: Yb:CNGG and Yb:CLNGG," Appl. Phys. B **109**(2), 183–188 (2012).
3. M. D. Serrano, J. O. Á.-Pérez, C. Zaldo, J. Sanz, I. Sobrados, J. A. Alonso, C. Cascales, M. F. Díaz, and A. Jezowski, "Design of Yb 3+ optical bandwidths by crystallographic modification of disordered calcium niobium gallium laser garnets," J. Mater. Chem. C **5**(44), 11481–11495 (2017).
4. Yu K. Voron'ko, A. B. Kudryavtsev, N. A. Es' kov, V. V. Osiko, A. A. Sobol, E. V. Sorokin, and F. M. Spiridonov, "Raman scattering of light in crystals and melt of calcium-niobium gallium garnet," *in Dokl. Akad. Nauk SSSR* 604–607 (1988).
5. A. Schmidt, U. Griebner, H. Zhang, J. Wang, M. Jiang, J. Liu, and V. Petrov, "Passive mode-locking of the Yb:CNGG laser," Opt. Commun. **283**(4), 567–569 (2010).
6. Y. Zhang, V. Petrov, U. Griebner, X. Zhang, S. Choi, J. Gwak, F. Rotermund, X. Mateos, H. Yu, H. Zhang, and J. Liu, "90-fs diode-pumped Yb:CLNGG laser mode-locked using single-walled carbon nanotube saturable absorber," Opt. Express **22**(5), 5635–5640 (2014).
7. Y. Zhang, V. Petrov, U. Griebner, X. Zhang, H. Yu, H. Zhang, and J. Liu, "Diode-pumped SESAM mode-locked Yb:CLNGG laser," Opt. Laser Technol. **69**, 144–147 (2015).
8. J. Á. Pérez, J. M. C. Cano-Torres, A. Ruiz, M. D. Serrano, C. Cascales, and C. Zaldo, "A roadmap for laser optimization of Yb: Ca3(NbGa)5O12-CNGG-type single crystal garnets," J. Mater. Chem. C **9**(13), 4628–4642 (2021).
9. J. Ma, Z. Pan, J. Wang, H. Yuan, H. Cai, G. Xie, L. Qian, D. Shen, and D. Tang, "Generation of sub-50fs soliton pulses from a mode-locked Yb,Na:CNGG disordered crystal laser," Opt. Express **25**(13), 14968–14973 (2017).

Optics EXPRESS

10. D. H. Sutter, G. Steinmeyer, L. Gallmann, N. Matuschek, F. Morier-Genoud, U. Keller, V. Scheuer, G. Angelow, and T. Tschudi, "Semiconductor saturable-absorber mirror–assisted Kerr-lens mode-locked Ti: sapphire laser producing pulses in the two-cycle regime," Opt. Lett. **24**(9), 631–633 (1999).
11. Y. Wang, X. Su, Y. Xie, F. Gao, S. Kumar, Q. Wang, C. Liu, B. Zhang, B. Zhang, and J. He, "17.8 fs broadband Kerr-lens mode-locked Yb:CALGO oscillator," Opt. Lett. **46**(8), 1892–1895 (2021).
12. H. Zeng, H. Lin, Z. Lin, L. Zhang, Z. Lin, G. Zhang, V. Petrov, P. Loiko, X. Mateos, L. Wang, and W. Chen, "Diode-pumped sub-50-fs Kerr-lens mode-locked Yb:GdYCOB laser," Opt. Express **29**(9), 13496–13503 (2021).
13. Z. Lin, H. Zeng, G. Zhang, W. Xue, Z. Pan, H. Lin, P. Loiko, H. Liang, V. Petrov, X. Mateos, L. Wang, and W. Chen, "Kerr-lens mode-locked Yb:SrLaAlO4 laser," Opt. Express **29**(26), 42837–42843 (2021).
14. P. Sévillano, P. Georges, F. Druon, D. Descamps, and E. Cormier, "32-fs Kerr-lens mode-locked Yb:CaGdAlO4 oscillator optically pumped by a bright fiber laser," Opt. Lett. **39**(20), 6001–6004 (2014).
15. Z. Gao, J. Zhu, J. Wang, Z. Wei, X. Xu, L. Zheng, L. Su, and J. Xu, "Generation of 33 fs pulses directly from a Kerr-lens mode-locked Yb:CaYAlO4 laser," Photonics Res. **3**(6), 335–338 (2015).
16. J. Ma, F. Yang, W. Gao, X. Xiaodong, X. Jun, D. Shen, and D. Tang, "Sub-five-optical-cycle pulse generation from a Kerr-lens mode-locked Yb:CaYAlO4 laser," Opt. Lett. **46**(10), 2328–2331 (2021).
17. R. Adair, L. L. Chase, and S. A. Payne, "Nonlinear refractive index of optical crystals," Phys. Rev. B **39**(5), 3337–3350 (1989).
18. Y. K. Voronko, A. A. Sobol, A. Y. Karasik, N. A. Eskov, P. A. Rabochkina, and S. N. UshakovCalcium niobium gallium and calcium lithium niobium gallium garnets doped with rare earth ions - effective laser media," Opt. Mater. **20**(3), 197 (2002).
19. V. Lupei, A. Lupei, C. Gheorghe, L. Gheorghe, A. Achim, and A. Ikesue, "Crystal field disorder effects in the optical spectra of Nd3+ and Yb3+-doped calcium lithium niobium gallium garnets laser crystals and ceramics," J. Appl. Phys. (Melville, NY, U. S.) **112**(6), 063110 (2012).
20. J. A. Caird, S. A. Payne, P. R. Staver, A. Ramponi, and L. Chase, "Quantum electronic properties of the Na3Ga2Li3F12: Cr3+ laser," IEEE J. Quantum Electron. **24**(6), 1077–1099 (1988).
21. J. M. Serres, V. Jambunathan, P. Loiko, X. Mateos, H. Yu, H. Zhang, J. Liu, A. Lucianetti, T. Mocek, K. Yumashev, U. Griebner, V. Petrov, M. Aguilo, and F. Diaz, "Microchip laser operation of Yb-doped gallium garnets," Opt. Mater. Express **6**(1), 46–57 (2016).
22. N. L. Boling, A. Glass, and A. Owyoung, "Empirical relationships for predicting nonlinear refractive index changes in optical solids," IEEE J. Quantum Electron. **14**(8), 601–608 (1978).
23. Z. Pan, Y. Wang, Y. Zhao, M. Kowalczyk, J. Sotor, H. Yuan, Y. Zhang, X. Dai, H. Cai, J. E. Bae, F. Choi, F. Rotermund, P. Loiko, J. M. Serres, X. Mateos, U. Griebner, and V. Petrov, "Sub-80 fs mode-locked Tm, Ho-codoped disordered garnet crystal oscillator operating at 2081nm," Opt. Lett. **43**(20), 5154–5157 (2018).